Electronic Supplementary Material (ESI) for Journal of Materials Chemistry A.

Supplementary Information

Developing diluted low-concentration electrolyte with high anion-to-solvent ratio for high-voltage lithium metal batteries

Chengzong Li[a], Yan Li[a], Yan Wang[a], Fengwei Bai[a], Xiang Chen[b], and Tao Li*[a]

[a] School of Resource Environment and Safety Engineering, University of South China, Hengyang 421001, P. R. China. E-mail address: li-tao@usc.edu.cn

[b] Department of Chemical Engineering, Tsinghua University, Beijing 100084, P. R. China.

Experimental section

Electrolyte preparation. Lithium bis(fluorosulfonyl)imide (LiFSI, 99.8%, DodoChem, Suzhou, China), 1,2-dimethoxyethane (DME, 99.95%, DodoChem, Suzhou, China), 1,1,2,2-tetrafluoroethyl-2,2,2-trifluoroethyl ether (HFE, 99%, Aladdin), 1,1,2,2-tetrafluoroethyl-2,2,3,3-tetrafluoropropyl ether (TTE, 99.8%, DodoChem, Suzhou, China), 1,1,1-trifluoro-2-(2,2,2-trifluoroethoxy)ethane (BTFE, 99.0%, TCI), 1,1,1, 3,3,3-hexafluoro-2-methoxypropane (HFME, >98%, Aladdin), fluorobenzene (FB, 99%, Aladdin), 1,2-difluorobenzeneand (1,2dFB, >98%, Aladdin), hexafluorobenzene (HFB, >99%, Aladdin), 2,2,2-trifluoroethyl trifluoromethanesulfonate (TFEOTF, 95%, Aladdin), ethyl 1,1,2,2-tetrafluoroethyl ether (ETE, 97%, Aladdin), aethyloxypentafluorcyclotriphosphazen (PFPN, >98%, Aladdin), (trifluoromethyl)benzene (BZTF, 99%, Aladdin), (trifluoromethoxy) benzene (TFMB, 98%, Aladdin), 1-fluoro(trifluoromethoxy)benzene (1, F-TFMB, 98%, Aladdin), (difluoromethoxy)benzene (DFMB, 98%, Aladdin), 2H,3H-Decafluoropentane (HFTC, >98%, Aladdin). The LCE was formulated by dissolving 0.5 M LiFSI in DME. The TTE-based LHCE was formulated by dissolving 2 M LiFSI in DME/TTE (1:1.2:2.3 by mol.). The commercial carbonate electrolyte was formulated by dissolving 1 M $LiPF_6$ in EC/DMC (1:1 by vol.). The electrolyte was prepared by dissolving the lithium salt into the requested solvent with a molar ratio, while the preparation process was carried out in an Ar-filled glove box, in which the content of O_2 and H_2O was strictly maintained at less than 1 ppm.

Electrode preparation. Li foils (30 μm in thickness) were ordered from China Energy Lithium Co., Ltd. $LiNi_{0.5}Co_{0.2}Mn_{0.3}O_2$ (NCM523) cathode (~3.8 mAh cm^{-2}) was ordered from Guangdong Canrd New Energy Technology Co., Ltd. Li foils and NCM523 cathode were punched into disks of 14 and 12 mm in diameter, respectively.

Electrochemical measurements. All batteries were assembled using the 2032-type coin cell with a polypropylene (PP) separator (Celgard 2500). The CE test was conducted in Li | Cu half cells using Zhang's method [1]. Li | NCM523 coin cells were assembled in an argon-filled glovebox (Mikrouna, with $H_2O < 0.01$ ppm, $O_2 < 0.01$ ppm). An additional Al foil disc (19 mm) was first placed in the cathode case to avoid the corrosion of the stainless steel at high voltage. The amount of electrolyte in coin cells was 40 μL per cell. The charge/discharge tests of coin cells were performed in the voltage range from 2.8 to 4.3 V at 25°C. To analyze the high-temperature and low-temperature cyclability of Li | NCM523 full cells, cyclability tests were conducted under 55 and −20°C, respectively.

In the linear sweep voltammetry (LSV) test, the SP-PVDF/Al electrode was used as the working electrode, where the Li metal was used as the counter and reference electrodes. The voltage window was set with a scan rate of 0.5 mV s^{-1}. The electrochemical impedance spectroscopy (EIS) measurement was performed in a frequency range between 10^5 and 10^{-1} Hz with an AC signal amplitude of 5 mV. All Li | NCM523 batteries were tested at the end of the charged state. Cyclic voltammetry (CV) was performed on symmetric Li | Li cells to measure the exchange current density. A fixed sweep rate of 1.0 mV/s was employed within a voltage range from −200 to 200 mV. The selected voltage range from 50 to 100 mV in the linear region was used to calculate the exchange current density. The LSV, EIS, and CV tests were conducted on a CHI660E electrochemical workstation.

Characterizations. SEM images and EDS elemental mappings were taken with a TESCAN MIRA LMS scanning electron microscope at an acceleration voltage of 5 and 15 kV, respectively. The Li-metal anodes retrieved from cycled Li | NCM523 batteries were first washed with pure DME solvent at least three times to remove the residual electrolyte and then dried thoroughly in the glovebox. The Li-metal anodes were protected in an argon-filled container to avoid contact with air during the transferring process before SEM characterizations. The Raman spectra were measured by using a MicroRaman system (LabRAM HR spectrometer, Horiba) equipped with an Olympus BX microscope and an argon ion laser (633 nm). X-ray photoelectron spectroscopy (XPS) experiments were obtained on a PHI 5000 VersaProbe II scanning XPS microprobe equipped with Al Kα radiation and argon ion sputter. Ar^+ sputtering rate for the XPS depth-profiling calibrated on the SiO_2 surface was ∼5 nm/min.

Theoretical calculations. The energies of the highest occupied molecular orbital (HOMO) and the lowest unoccupied molecular orbital (LUMO) were calculated by the density functional theory (DFT) implanted in Gaussian 16 software.[2] Becke's three-parameter hybrid method using the Lee–Yang–Parr correlation functional (B3LYP) and 6-311++G(d, p) basis set were chosen to optimize the geometrical structures and for single-point calculations. The ESP of the solvent was analyzed by using Multiwfn software.[3]

Molecular dynamics (MD). Molecular dynamics (MD) calculations were conducted using a Material Studio (BIOVIA, 2020) software package. Geometries of the DME, Li^+, FSI^-, and TFMB species were optimized using the forcite module. A condensed-phase optimized molecular potential for atomistic simulation studies III (COMPASS III) forcefield was assigned for all the MD calculations. The solvation sheath components of the co-salt electrolytes were estimated by constructing amorphous cells with 30 FSI^-, 30 Li^+, and x:y ratios of DME and TFMB (x:y = 72:398, 48:415, and 36:426), the ratio of which corresponds to the actual electrolyte of 4 M-0.5 M, 6 M-0.5 M and 8 M-0.5 M. The systems were in cubic boxes with the same dimensions of 49 Å in length, width, and height. All the systems were initially stabilized for 50000 steps using the smart algorithm employing an energy convergence tolerance of 0.001 kcal mol^{-1} $Å^{-1}$. Following the energy minimization, the electrolyte systems were equilibrated for 1 ns in the MD simulations using a time step of 1 fs in the isobaric-isothermal (NPT) ensemble. The Berendsen barostat was used with maintaining a pressure of 1 atm with a decay constant of 0.1 ps. Subsequently, the systems were run for 1 ns in a canonical NVE ensemble at 298 K and run for 5 ns in a canonical NVT ensemble at 298 K. The radial distribution functions (RDFs) were calculated based on the last 5 ns productions.

Supplementary figures

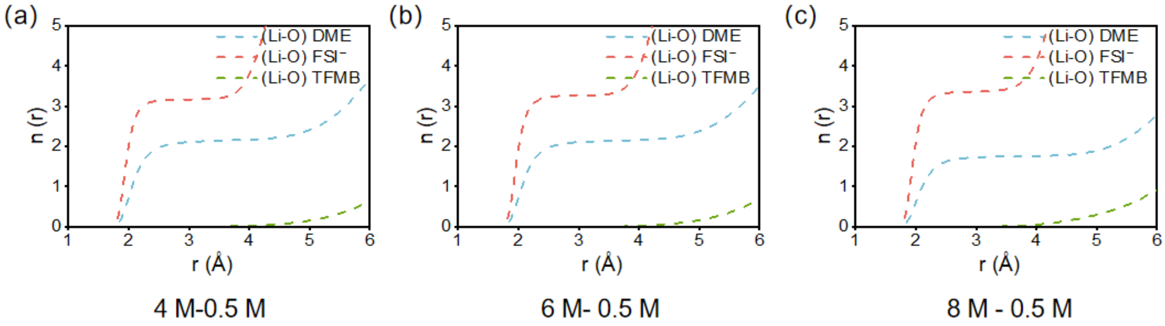

Fig. S1 Coordination numbers (dashed lines) of Li−O (DME), Li−O (FSI$^-$), and Li−O (TFMB) pairs in (a) 4 M-0.5 M, (b) 6 M-0.5 M, and (c) 8 M-0.5 M electrolytes.

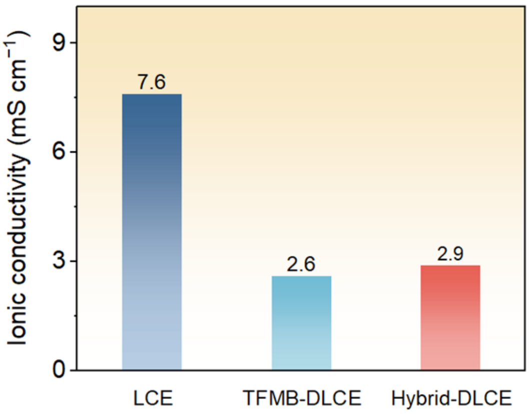

Fig. S2 Ionic conductivity of different electrolytes. LCE (0.5 M LiFSI in DME).

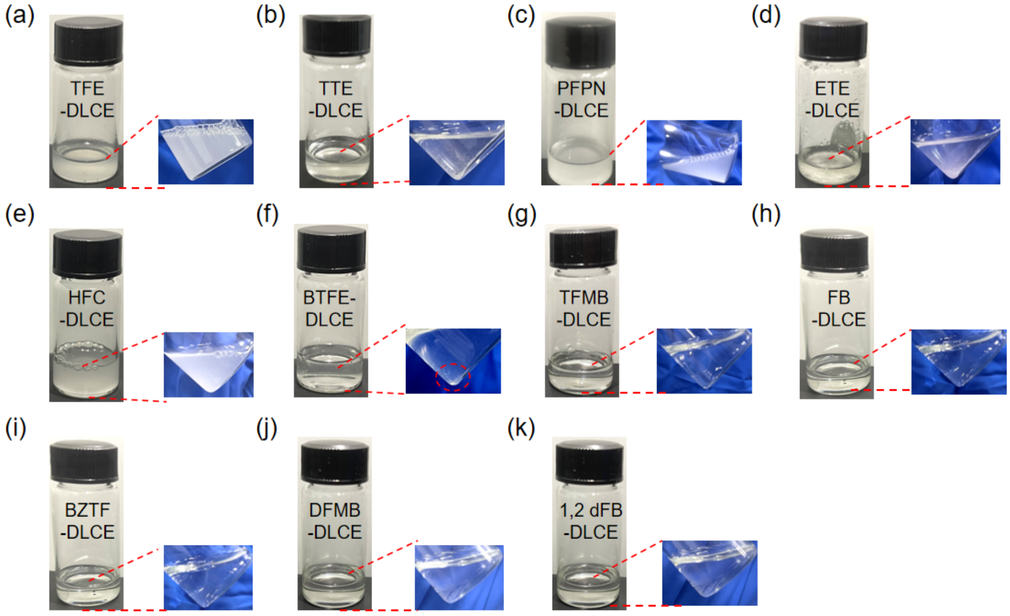

Fig. S3 Photos of DLCEs diluted from 8.0 M to 0.5 M with various diluents.

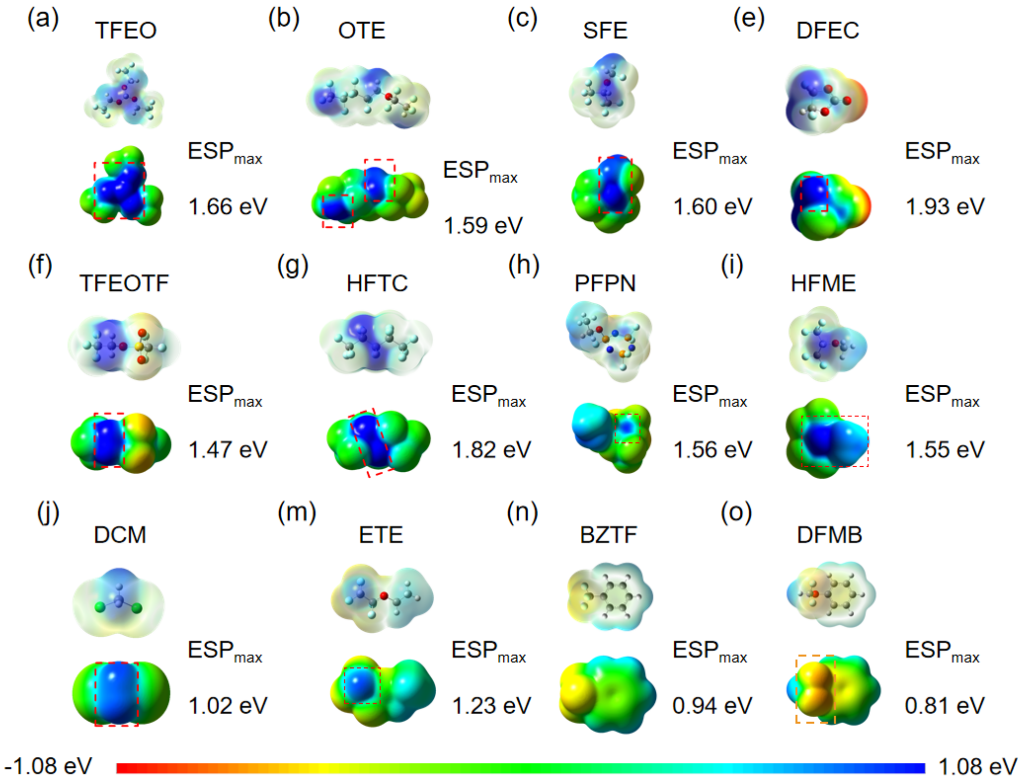

Fig. S4 Calculated electrostatic potential maps of diluents under vacuum conditions. O, H, S, N, P, C and F atoms are shown in red, white, yellow, blue, orange, black and light sky blue, respectively. Isovalue＝0.02.

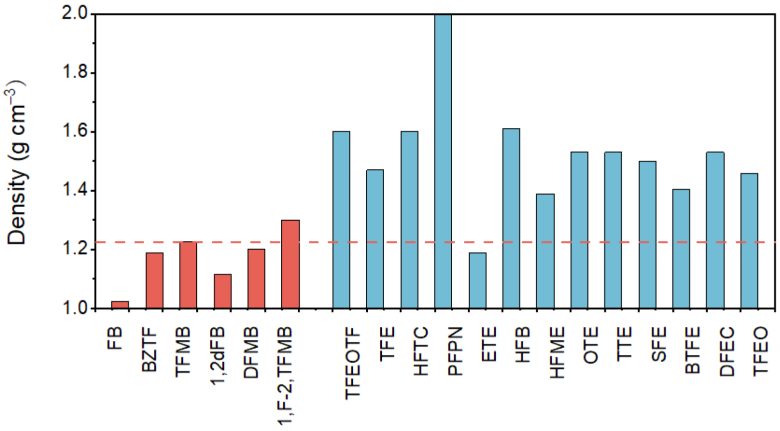

Fig. S5 Density comparison of various diluents.

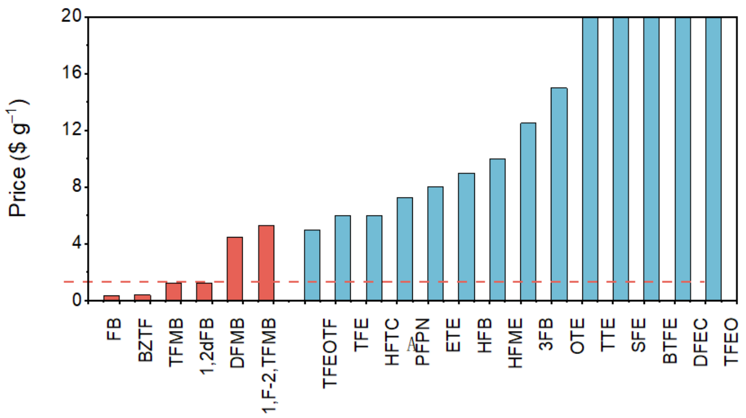

Fig. S6 Cost comparison of different diluents.

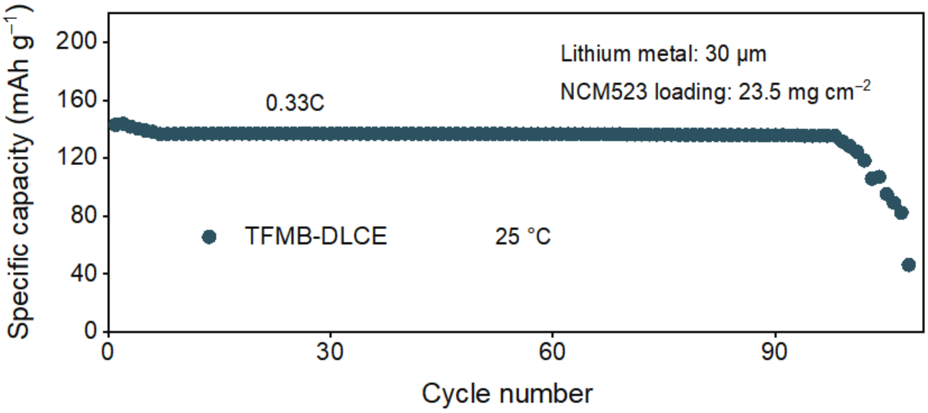

Fig. S7 Cycling performance of Li | NCM523 cells with TFMB-DLCE at 4.3 V/0.33 C.

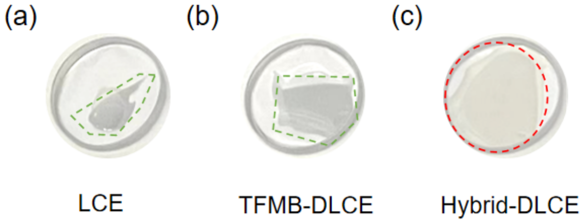

Fig. S8 Wettability of different electrolytes to separator. (a) LCE. (b) TFMB-DLCE and (c) hybrid-DLCE.

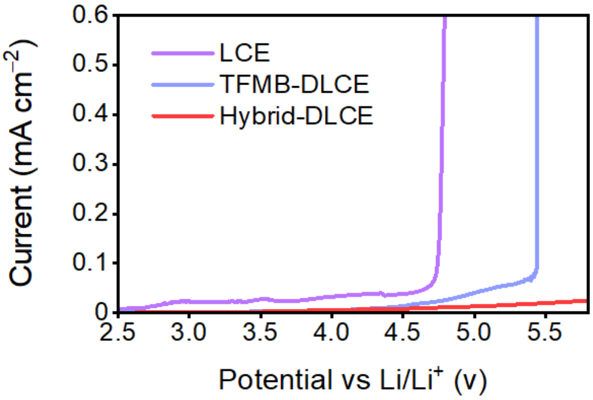

Fig. S9 LSV curves of LCE, TFMB-DLCE, and hybrid-DLCE at a scanning rate of 0.5 mV s^{-1}.

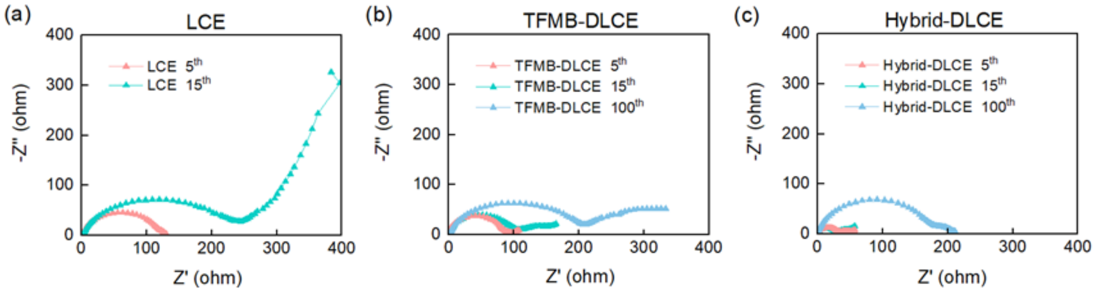

Fig. S10 The evolutions of interfacial resistance of Li | NCM523 batteries with (a) LCE, (b) TFMB-DLCE and (c) hybrid-DLCE.

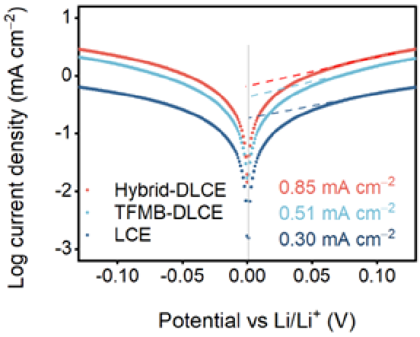

Fig. S11 Tafel polt of different electrolytes.

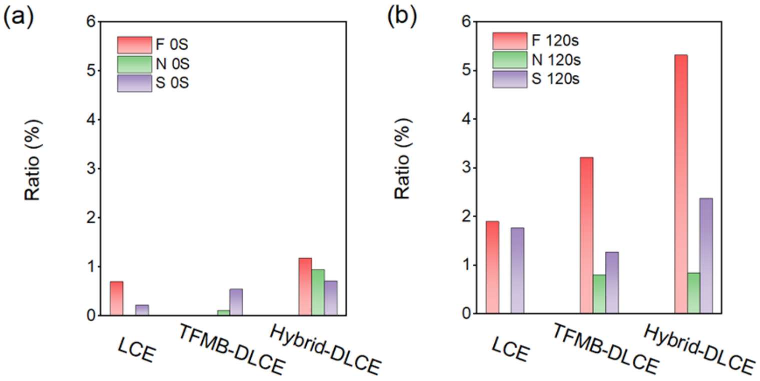

Fig. S12 SEI components information obtained by XPS measurements: (a,b) F, N, and S contents before and after 120 s of sputtering.

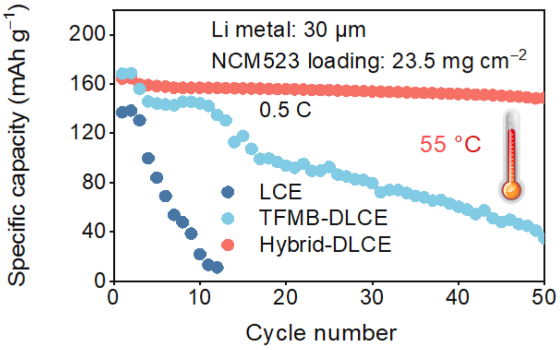

Fig. S13 Cycling performance of Li | NCM523 cells with different electrolytes at 4.3 V/55°C.

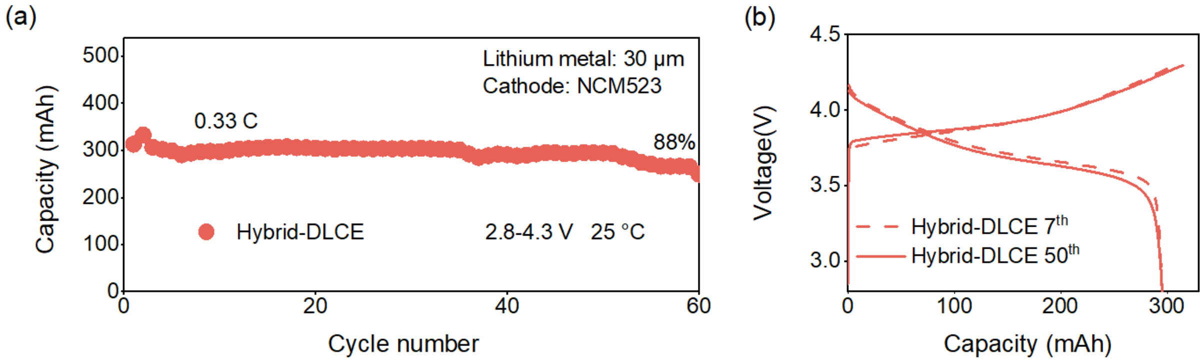

Fig. S14 (a) Cycling performance of Li | NCM pouch cell with hybrid-DLCE at 0.33 C after two formation cycles. (b) Voltage profiles of Li | NCM pouch cell with hybrid-DLCE from 7th to 50th cycles.

Supplementary tables

Table S1. The full name and abbreviation of diluents mentioned in this work.

Diluent	Abbreviation	Diluent	Abbreviation
1,1,2,2- tetrafluoroethyl-2,2,2-trifluoroethyl ether	HFE	Fluorobenzene	FB
1,1,2,2-tetrafluoroethyl 2,2,3,3-tetrafluoropropyl ether	TTE	1,2-difluorobenzene	1,2dFB
Bis(2,2,2trifluoroethyl) ether	BTFE	Hexafluorobenzene	HFB
1H,1H,5Hoctafluoropentyl 1,1,2,2-tetrafluoroethyl ether	OTE	(Trifluoromethoxy)benzene	TFMB
Dichloromethane	DCM	(Trifluoromethyl)benzene	BZTF
Ethyl 1,1,2,2-tetrafluoroethyl ether	ETE	(Difluoromethoxy)benzene	DFMB
Hexafluoroisopropyl methyl ether	HFME	2H,3H-Decafluoropentane	HFTC
sevoflurane	SFE	Aethyloxypentafluorcyclotriphosphazen	PFPN
Tris[(trifluoroethoxy)methane]	TFEO	1,3-Dioxolan-2-one,4,5-difluoro	DFEC

Table S2. Molecular formula and physical properties of three diluents.

	TFMB	ETE	PFPN
Molecular formula	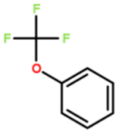	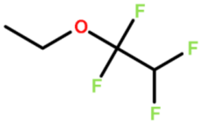	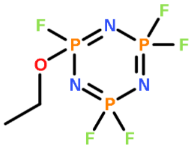
Boiling point (°C)	102	57	125
Melting point (°C)	−50	−86	−34
Flash point (°C)	12	−15	/
Density (g ml^{-1})	1.23	1.19	2.08

Table S3. Comparison of electrochemical performance of current advanced electrolytes for high-voltage Li metal batteries.

	Capacity （mAh cm^{-2}）	Voltage (V)	cycle	Rate	Li thickness (μm)	Ref.
This work	4.3	4.5	120	0.4 C	30	/
	3.8	4.3	180	1 C	30	/
0.5 M $LiPF_6$	2.8	4.3	150	0.33 C	30	Ref.38
0.5 M LiFSI	3.6	4.3	50	/	0	Ref.50
0.25 M dual-salt	0.6	4.3	150	0.5 C	50	Ref.45
0.3 M LiFSI	0.5	3.6	100	2 C	/	Ref.40
0.5 M dual-salt	2	3.8	300	/	450	Ref.46
0.5 M multi-salt	2.6	4.3	300	0.5 C	/	Ref.49
0.2 M $LiPF_6$	0.5	4.35	300	0.5 C	450	Ref.44
0.25 M dual-salt	1.28	4.3	100	0.3 C	400	Ref.48
0.5 M dual-salt	4.5	4.6	120	0.22 C	50	Ref.37
0.25 M LiFSI	1.79	4.1	100	1 C	/	Ref.47

Table S4. Interfacial resistance of Li | NCM523 batteries in LCE, TFMB-DLCE, and hybrid-DLCE at different cycles.

	5th cycle resistance (Ω)		15th cycle resistance (Ω)		100th cycle resistance (Ω)	
	R_{SEI}	R_{ct}	R_{SEI}	R_{ct}	R_{SEI}	R_{ct}
LCE	109.0	20.9	241.1	139.1		
TFMB-DLCE	98.0	10.1	106.7	58.3	206.9	124.1
Hybrid-DLCE	30.5	26.8	35.7	22.5	171.4	40.0

References

1. B. D. Adams, J. Zheng, X. Ren, W. Xu and J.-G. Zhang, *Adv. Energy Mater.,* 2018, 8*,* 1702097.
2. M. J. T. Frisch, G. W.; Schlegel, H. B.; Scuseria, G. E.; Robb, M. A.; Cheeseman, J. R.; Scalmani, G.; Barone, V.; Petersson, G. A.; Nakatsuji, H.; Li, X.; Caricato, M.; Marenich, A. V.; Bloino, J.; Janesko, B. G.; Gomperts, R.; Mennucci, B.; Hratchian, H. P.; Ortiz, J. V.; Izmaylov, A. F.; Sonnenberg, J. L.; Williams-Young, D.; Ding, F.; Lipparini, F.; Egidi, F.; Goings, J.; Peng, B.; Petrone, A.; Henderson, T.; Ranasinghe, D.; Zakrzewski, V. G.; Gao, J.; Rega, N.; Zheng, G.; Liang, W.; Hada, M.; Ehara, M.; Toyota, K.; Fukuda, R.; Hasegawa, J.; Ishida, M.; Nakajima, T.; Honda, Y.; Kitao, O.; Nakai, H.; Vreven, T.; Throssell, K.; Montgomery, J. A., Jr.; Peralta, J. E.; Ogliaro, F.; Bearpark, M. J.; Heyd, J. J.; Brothers, E. N.; Kudin, K. N.; Staroverov, V. N.; Keith, T. A.; Kobayashi, R.; Normand, J.; Raghavachari, K.; Rendell, A. P.; Burant, J. C.; Iyengar, S. S.; Tomasi, J.; Cossi, M.; Millam, J. M.; Klene, M.; Adamo, C.; Cammi, R.; Ochterski, J. W.; Martin, R. L.; Morokuma, K.; Farkas, O.; Foresman, J. B.; Fox, D. J.Gaussian 16, Revision B.01, Gaussian, Inc., Wallingford CT, 2016.
3. T. Lu and F. Chen, *J. Comput. Chem.,* 2012, 33*,* 580–592.